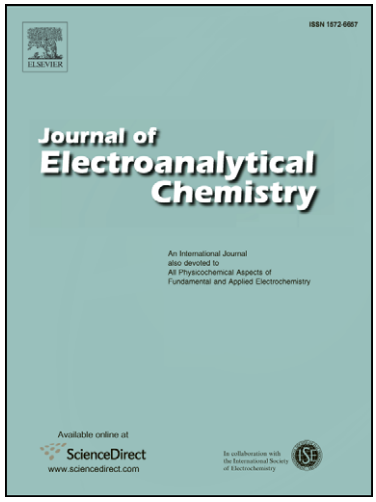

Phenol And *Para*-Substituted Phenols Electrochemical Oxidation Pathways

Teodor Adrian Enache, Ana Maria Oliveira-Brett

PII: S1572-6657(11)00105-6
DOI: 10.1016/j.jelechem.2011.02.022
Reference: JEAC 439

To appear in: *Journal of Electroanalytical Chemistry*

Received Date: 5 November 2010
Revised Date: 18 February 2011
Accepted Date: 20 February 2011

Please cite this article as: T.A. Enache, A.M. Oliveira-Brett, Phenol And *Para*-Substituted Phenols Electrochemical Oxidation Pathways, *Journal of Electroanalytical Chemistry* (2011), doi: 10.1016/j.jelechem.2011.02.022

PHENOL AND *PARA*-SUBSTITUTED PHENOLS

ELECTROCHEMICAL OXIDATION PATHWAYS

Teodor Adrian Enache and Ana Maria Oliveira-Brett*

Departamento de Química, Faculdade de Ciências e Tecnologia, Universidade de Coimbra, 3004-535 Coimbra, Portugal

* To whom correspondence should be addressed

Tel: +351-239-835295

e-mail: brett@ci.uc.pt

Departamento de Quíımica,

Faculdade de Ciências e Tecnologia,

Universidade de Coimbra,

3004-535 Coimbra, Portugal

ABSTRACT

The electrochemical behaviour of phenol, catechol, hydroquinone, resorcinol, dopamine, and *para*-substituted phenolic compounds, 4-ethylphenol, tyrosine, and tyramine, was studied over a wide pH range using a glassy carbon electrode. The oxidation of phenol is pH dependent and irreversible, occurring in one step, and followed by hydrolyse in *ortho*- and *para*- positions, leading to two oxidation products, catechol and hydroquinone. The oxidation of phenol oxidation products, *ortho*-phenol and *para*-phenol, is reversible and pH dependent. The oxidation potential of *para*-substituted phenols varies slightly due to their substituent group in position C4, and occurs in one oxidation step corresponding to the oxidation of phenol. The oxidation products of this group of *para*-substituted phenols are reversibly oxidised and adsorb on the electrode surface.

Keywords: phenol, *para*-substituted phenols, voltammetry, oxidation, glassy carbon

1. INTRODUCTION

Phenolic compounds represent a large group of biological molecules with a variety of functions in plant growth, development, and defence. Phenolic compounds are a class of chemical compounds consisting of a hydroxyl functional group (─OH) attached to an aromatic hydrocarbon group, with a ring structure like that of benzene. They are also related to the groups of hormones, vitamins, amino acids and antioxidants [1]. Pharmacological studies of phenolic compounds have reported a wide variety of important biological properties such as anti-inflammatory, antibacterial, anticonvulsant, antitumour and antioxidant properties [1-8].

These compounds donate hydrogen and the mechanism of their action as antioxidants involves the ability of phenols to scavenge radicals by an H-atom or electron transfer process by which the phenol is converted into a phenoxyl radical [9, 10]. The resulting antioxidant free radical does not lead to formation of another free radical due to the stabilization by delocalization of radical electron [2].

Several phenols such as tyrosine and tyramine are the building blocks of numerous natural products, including dityrosine, L-dopa and dopamine, and the biosynthesis of these compounds, by oxidative coupling, seems to proceed via a phenoxyl radical [11].

Investigations of the redox behavior of biologically occurring compounds by means of electrochemical techniques have the potential for providing valuable insights into the biological redox reactions of these molecules. Due to their high sensitivity, voltammetric methods have been successfully used to study the redox behavior of various biological compounds. The redox behaviour of phenol derivatives has already been reported at different electrode materials: gold [12, 13], platinum [12, 13, 14],

carbon [13, 15, 16, 17, 18, 19], boron doped diamond [20, 21, 22], mercury drop [23] and Ti/IrO_2 [24].

Hydroquinone, phenol and benzoquinone species were identified after HPLC analysis of a solution in which phenol was electrolyzed, using a carbon black slurry electrode [18]. The direct oxidation of phenol at a boron doped diamond electrode [21], in the potential region of water stability, and the indirect oxidation reaction which takes place via electrogenerated hydroxyl radicals active intermediate species, at high applied potentials, was described. Moreover, the complete combustion of phenol to CO_2 was possible or the partial oxidation of phenol to other aromatic compounds, benzoquinone, hydroquinone and catechol, depending on the values of applied current and phenol concentration [21].

Two oxidation mechanisms were proposed for the electrochemical oxidation of tyrosine. The main oxidation product obtained at high concentrations was characterized as an inhibitor polymeric film, and at low concentrations the oxidation of tyrosine occurred without polymerization [12, 13].

Although several mechanisms regarding the oxidation of phenol and phenol derivatives were described, more work needs to be done to fully characterize the electrochemical oxidation reactions of these compounds.

The present study is concerned with the investigation of the electron transfer properties of phenol, catechol, hydroquinone, resorcinol, dopamine, and *para*-substituted phenolic compounds, 4-ethylphenol, tyrosine, and tyramine, using differential pulse and square wave voltammetry at glassy carbon electrode in order to clarify the redox mechanisms of natural or synthetic phenols, and the results will provide a contribution to the understanding of their quantitative structure activity relations (QSAR).

2. EXPERIMENTAL

2.1 Materials and reagents

The phenolic compounds, phenol, catechol, hydroquinone, resorcinol, 4-ethylphenol, tyrosine, tyramine and dopamine, **Scheme 1,** were obtained from Sigma and were used without further purification. Stock solutions of 1 mM were prepared in deionized water and were stored at 4 ºC.

All supporting electrolyte solutions, **Table 1**, were prepared using analytical grade reagents and purified water from a Millipore Milli-Q system (conductivity ≤ 0.1 μS cm^{-1}).

Microvolumes were measured using EP-10 and EP-100 Plus Motorized Microliter Pippettes (Rainin Instrument Co. Inc., Woburn, USA). The pH measurements were carried out with a Crison micropH 2001 pH-meter with an Ingold combined glass electrode. All experiments were done at room temperature (25 ± 1 ºC).

2.2 Voltammetric parameters and electrochemical cells

Voltammetric experiments were carried out using a μAutolab running with GPES 4.9 software, Eco-Chemie, Utrecht, The Netherlands. The experimental conditions for cyclic voltammetry (CV) was ν = 50 mV s^{-1}, and for differential pulse (DP) voltammetry were: pulse amplitude 50 mV, pulse width 70 ms, scan rate 5 mV s^{-1}. Measurements were carried out using a glassy carbon (GCE) (d = 1.5 mm) working

electrode, a Pt wire counter electrode, and a Ag/AgCl (3 M KCl) as reference electrode, in a 0.5 mL one-compartment electrochemical cell.

The GCE was polished using diamond spray (particle size 1 μm) before each experiment. After polishing, the electrode was rinsed thoroughly with Milli-Q water for 30s. After this mechanical treatment, the GCE was placed in pH 7 0.1 M phosphate buffer electrolyte and various DP voltammograms were recorded until a steady state baseline voltammogram was obtained. This procedure ensured very reproducible experimental results.

2.3 Acquisition and presentation of voltammetric data

All the voltammograms presented were background-subtracted and baseline-corrected using the moving average with a step window of 3 mV included in GPES version 4.9 software. This mathematical treatment improves the visualization and identification of peaks over the baseline without introducing any artefact, although the peak height is in some cases reduced (<10%) relative to that of the untreated curve. Nevertheless, this mathematical treatment of the original voltammograms was used in the presentation of all experimental voltammograms for a better and clearer identification of the peaks. The values for peak current presented in all graphs were determined from the original untreated voltammograms after subtraction of the baseline.

3. RESULTS AND DISCUSSION

The oxidation behaviour of phenol and *para*-substituted phenolic compounds was investigated by cyclic (CV), differential pulse (DP) and square wave (SW)

voltammetry at a glassy carbon electrode (GCE) in electrolytes with different pH values. In order to identify the oxidation pathway of phenol and *para*-substituted phenolic compounds, a comparative study between phenol and the benzenediol isomers, catechol, hydroquinone, resorcinol, was also performed.

3.1 Cyclic voltammetry of phenol

The cyclic voltammetric behaviour of phenol was carried out in a solution 30 μM phenol in pH 7.0 0.1 M phosphate buffer, saturated with N_2, **Figure 1**, and during the voltammetric measurement a constant flux of N_2 was kept over the solution surface in order to avoid the diffusion of atmospheric oxygen into the solution of phenol.

In these condition, phenol undergoes oxidation in a single step, peak 1_a, at E_{p1a} = + 0.71 V. On the negative-going scan, two reduction peaks occurred peak 3_c, at E_{p3c} = + 0.40 V, and peak 2_c, at E_{p2c} = + 0.29 V. The cathodic peaks correspond to the reduction of the two phenol oxidation products, *ortho*-quinone to *ortho*-phenol (catechol), peak 3_c, and *para*-quinone to *para*-phenol (hydroquinone), peak 2_c, **Scheme 2A**. The second CV scanning in the positive direction, in the same solution and without cleaning the GCE surface, showed two anodic peaks: peak 2_a at E_{p2a} = + 0.33 V, and peak 3_a, at E_{p3a} = + 0.43 V, indicating the reversibility of peaks 2_c and 3_c. The differences between the anodic and the cathodic peak potentials, $|E_{p2a} - E_{p2c}|$ = 40 mV and $|E_{p3a} - E_{p3c}|$ = 30 mV, close to the theoretical value of 30 mV for a two-electron reversible reaction, confirm the reversibility of both peaks [25]. At the same time, a decrease current of peak 1_a, due to the adsorption of phenol oxidation products, on the GCE surface was also observed. Hydroquinone oxidation peak 2, catechol oxidation peak 3,

and *para*-quinone and *ortho*-quinone adsorb on the GCE surface forming a non-compact monolayer. Further oxidation of phenol molecules diffusing from the bulk solution towards the electrode, is more difficult because it occurs through the layer of adsorbed *para*- and *ortho*-phenol.

3.2 Diferential pulse voltammetry

3.2.1 Phenol

The DP voltammograms of supporting electrolyte pH 7.0 0.2 M phosphate buffer and 25 μM phenol: first and second scan, and DP voltammograms baseline-corrected, first and second scan, are presented in **Figure 2**, to demonstrate that the baseline-correction does not affect the results, but enables a better and clearer identification of the peaks obtained in the untreated voltammograms.

The DP voltammograms, **Figure 3A**, were all recorded at a clean GCE in solutions of 25 μM phenol in different pH electrolytes with 0.1 M ionic strength.

In all pHs the phenol oxidation occurred in a single step corresponding to oxidation peak 1_a. The oxidation potential of peak 1_a, occurring at E_p = + 1.02 V in pH 1.0, is pH dependent. The pH dependence is linear following the relationship E_p (V) = 1.02 – 0.060 pH, **Figure 3B.** The slope of the dotted line, 60 mV per pH unit, showed that the oxidation of phenol at GCE, in aqueous media, involves the same number of electrons and protons [25]. Taking into consideration the width at half height of peak 1_a, $W_{1/2}$ ~ 100 mV, it can be concluded that phenol oxidation process involves the transfer of one electron and one proton, and that the peak current has a maximum in neutral electrolytes, **Figure 3B**.

Successive DP voltammograms were recorded in a solution of 25 μM phenol in pHs between 1.0 and 12.0. On the second DP scan, recorded in the same solution and

without cleaning the GCE, the two anodic peaks 2_a and 3_a appeared. These peaks correspond to the oxidation of phenol oxidation products, *ortho*-phenol and *para*-phenol, **Scheme 2A**. The current of peak 1_a decreased with the number of scans due to the decrease of the available electrode surface area owing to adsorption of phenol oxidation products.

The electrochemical behavior of phenol oxidation products at the GCE surface was also studied for different pH values. After two consecutive DP voltammograms in 25 μM phenol solution in different pH buffer electrolytes, the results for the second DP voltammograms were plotted vs. pH, **Figure 4A**.

Peaks 2_a and 3_a were pH dependent, their potential decreasing linearly with the pH of the supporting electrolyte, **Figure 4B**. In both cases, the slope of the dotted lines was 60 mV per pH unit, meaning that the number of protons transferred during the oxidation of phenol oxidation product is equal with the number of electrons [25]. The peak width at half height varied between 55 and 65 mV for both peaks corresponding to the transfer of two electrons. Thus, the oxidation mechanism of phenol oxidation products involves the transfer of two electrons and two protons, and the current of the oxidation peaks of phenol oxidation products has a maximum in neutral electrolytes, **Figure 4B**.

Two shoulders were observed in the second DP voltammogram recorded in a solution of 25 μM phenol in pHs between 1.0 and 12.0, one before peak 2 and another after peak 3, **Figure 4**. The shoulders of peaks 2 and 3 are due to functional groups of the glassy carbon electrode [26]. Hydroquinone oxidation peak 2, catechol oxidation peak 3, and para-quinone and ortho-quinone adsorb on the GCE surface forming a non-compact monolayer. Further oxidation of catechol molecules diffusing from the bulk

solution towards the electrode, is more difficult because it occurs through the layer of adsorbed para- and ortho-phenol.

3.2.2 Phenol, hydroquinone, catechol and resorcinol

The electrochemical oxidation of phenol and the benzenediol isomers, hydroquinone, catechol and resorcinol, was studied by DP voltammetry in solutions of 25 μM in pH 7 0.1 M phosphate buffer, **Figures 5A-5C**. For each compound, two consecutive DP voltammograms were recorded between +0.0 V and + 1.0 V in a fresh solution at a clean GCE surface.

In these conditions the phenol oxidation peak 1_a occurred at E_p = + 0.65 V, involving a mechanism with the transfer of one electron and one proton (Section 3.2.1), and the phenol oxidation products peaks 2_a, at E_{p2a} = + 0.07 V, and peak 3_a, at E_{p3a} = + 0.30 V, **Figure 5A**.

The electrochemical behavior of hydroquinone is very similar to catechol, **Figures 5B and 5C**. For both isomers, only one anodic peak 1_a was obtained in first DP voltammograms, for hydroquinone, at E_p = + 0.08V, and for catechol, at E_p = + 0.20V. Whereas resorcinol oxidation occurs at a higher potential E_p = + 0.60V, **Figure 5D.** All oxidation peak currents decrease slightly with the number of scans.

It is well know that hydroquinone and catechol undergo reversible oxidation to quinone by a transfer of two electrons and two protons [27], and that the *meta*-quinone compound generated in the first stage of the electro-oxidation of resorcinol is not thermodynamically stable. The higher oxidation potential of resorcinol relative to hydroquinone or catechol is explained by the differences in reactivity of these isomers. The reactivity of the aromatic ring activated with an OH group increases when the OH group is in the *ortho* or *para* positions since the highest electron density is located on

both *ortho* and *para* positions Therefore, hydroquinone and catechol have the aromatic ring activated, while the resorcinol ring is not activated.

3.2.3 Para-substituted phenols and dopamine

In order to determine the electroactive centres of *para*-substituted phenols, 4-ethylphenol, tyramine and tyrosine, experiments were carried out and the results were compared with those obtained in the electrochemical oxidation of dopamine, the hydroxylation product of tyramine.

The electrochemical behavior of 4-ethylphenol, tyramine and tyrosine was studied at a GCE, using DP voltammetry, in solutions of 25 μM in pH 7 0.1 M phosphate buffer, **Figures 6A-6C**. The first and second voltammograms were recorded for each solution.

The first DP voltammograms recorded for all three *para*-substituted phenols, 4-ethylphenol, tyramine and tyrosine, between +0.0 V and + 1.0 V at a clean GCE presented one peak 1_a, at E_{p1a} ~ + 0.65V, at the same potential of the oxidation of peak 1_a of phenol. The potential of this peak varies slightly with the substituent at the position C4 of the *para*-substituted phenols, **Figures 6A-6C**.

In the first DP voltammograms recorded in a solution of 25μM dopamine in pH 7.0, two consecutive oxidation peaks, **Figure 6D,** were observed. The oxidation of the first peak 1_a, at E_p = + 0.18V, is attributed to the oxidation of the catechol group of dopamine in dopaminoquinone. For pH > 5, by Michael addition, dopaminoquinone lead to leucodopaminochrome [28]. Therefore, the oxidation of the second peak 2_a, at E_{p2a} = + 0.88V, corresponds to the oxidation of the leucodopaminochrome species formed in electrolytes with pH > 5.0.

The second DP voltammograms recorded for 4-ethylphenol, tyramine and tyrosine, in the same solutions and without cleaning the GCE, all showed the new oxidation peak 2_a, at a lower potential close to the value of the first oxidation peak 1_a of dopamine.

These experiments showed that the oxidation of 4-ethylphenol, tyramine and tyrosine, occurs by a similar one electron transfer mechanism followed by hydrolyse after the first oxidation product, and forming an oxidised catechol group in their quinone species, **Scheme 2B**. The oxidation of the *para*-substituted phenols oxidation products at peak 2_a corresponds to the oxidation of this catechol group.

The small differences in the oxidation potentials and currents observed between these compounds are due to the presence of different substituents in the *para* position of the phenol molecule but do not alter the oxidation pathways.

3.3 Square wave voltammetry

3.3.1 Phenol, hydroquinone, catechol and resorcinol

SW voltammograms recorded in a solution of 25 μM phenol in pH 7 0.1 M phosphate buffer, showed similar features to DP voltammetry, oxidation peak 1_a, at E_{p1a} = + 0.66 V, **Figure 7A,** and the second SW voltammogram showed two reversible peaks, peak 2_a, at E_{p2a} = +0.08V and peak 3_a, at E_{p3a} = +0.33V, corresponding to the oxidation of the oxidation products of phenol, **Figure 7B**.

A greater advantage of SWV is the possibility to see during only one scan if the electron transfer reaction is reversible or not [25]. Since the current is sampled in both positive and negative-going pulses, peaks corresponding to the oxidation and reduction

of the electroactive species at the electrode surface can be obtained in the same experiment.

Thus, the irreversibility of phenol oxidation peak 1_a was confirmed by plotting the forward and backward components of the total current, **Figure 7A**, and the forward component showed the peak at the same potential and with the same current as the total current obtained, and on the backward component no cathodic peak occurred.

The second SW voltammogram recorded in the solution phenol and without cleaning the GCE, showed the occurrence of two reversible peaks 2_a and 3_a, **Figure 7B**. Plotting the forward and backward components of the total current, the oxidation and the reduction currents and potentials showed a similar value which confirms the reversibility of both peaks. The peak potentials are identical to those of catechol, **Figure 7C**, and hydroquinone, **Figure 7D**, confirming the formation of dihydroxybenzene species in *ortho* e *para* position in the oxidation of phenol.

The first SW voltammogram in a solution of 25 μM resorcinol in pH 7.0 0.1 M phosphate buffer, shows an irreversible oxidation peak 1_a occurring at an oxidation potential similar with that of phenol, E_p = + 0.65 V, **Figure 7E,** that after undergoes hydrolysis. On the second SW voltammogram in resorcinol solution, without cleaning the GCE, a new peak 2_a appeared at a lower potential, E_p = + 0.08 V, **Figure 7F,** corresponding to the oxidation of resorcinol oxidation product. The new peak has an identical potential on the forward and backward components confirming the reversibility of the resorcinol oxidation products adsorbed on the GCE surface.

3.3.2 Tyramine and dopamine

The first SW voltammogram recorded in a solution of 25 μM tyramine in pH 7.0 0.1 M phosphate buffer, **Figure 8A,** showed similar features to the first SW

voltamogram recorded in a solution of phenol, the irreversible oxidation peak 1_a, at E_p = + 0.62 V, and in the second SW voltammogram the occurrence of peak 2_a, at E_p = + 0.20 V, **Figure 8B**.

The differences between the oxidation products of phenol and tyramine are explained because the *para-* position in the aromatic ring of tyramine is occupied. Plotting the forward and backward components of the total current, the oxidation and the reduction currents and potentials showed a similar value confirming the reversibility of peak 2_a, and the adsorption of tyramine oxidation product on the GCE surface.

The first SW voltammograms recorded in a solution of 25 μM dopamine in pH 7.0 0.1 M phosphate buffer, **Figure 8C**, showed a reversible peak 1_a, at E_p = + 0.20 V, which corresponds to the oxidation of the catechol group in this quinone species. The identical potential of reversible peak 2_a of tyramine and peak 1_a of dopamine indicates that after oxidation tyramine is hydrolysed to an oxidised catechol species.

3.4 Oxidation mechanisms of phenol and *para*-substituted phenol

The anodic behaviour of phenol was investigated using CV and DP voltammetry. The CV study, although not so sensitive as DP voltammetry, was very important as it enabled rapid screening of the reversibility of electron transfer processes occurring and of the formation of electroactive products. DP voltammetry was more sensitive than CV and very important to clarify the electron transfer processes, showing when they were coupled with simultaneous proton transfer and the formation of electroactive products.

In order to understand the redox mechanism of phenol, its electrochemical behaviour was compared with the electrochemical oxidation of the benzenediol isomers

hydroquinone, catechol and resorcinol. Phenol is oxidized in a one-electron and one proton step, peak 1_a, to a phenoxy radical which is not thermodynamically stable and can exist in three isomeric forms, **Scheme 2A**. The highest spin density of this radical is in the *ortho*- and *para*-positions. Therefore, the *meta* position is not favored for any kind of chemical reaction and is followed by stabilisation of the phenoxyl radical by hydrolysis at a high potential, phenol oxidation peak 1_a, resulting in the formation of two electroactive products, *ortho*-quinone and *para*-quinone. The two products are electrochemically reversibly reduced in a two-electron and two-proton mechanism, the *ortho*-quinone to catechol, peak 3_c, and the *para*-quinone to hydroquinone, peak 2_c.

Considering all the data presented, the electrochemical oxidation mechanism of phenol at GCE leads to two oxidation products, hydroquinone and catechol, and can be described by an electrochemical-chemical (EC) mechanism, **Scheme 2A**.

Taking into account the phenol EC mechanism, the oxidation pathways of *para*-substituted phenols is also explained by an EC mechanism, but only involving a catechol species, since their *para* position is always occupied in the substituted phenols, **Scheme 2B**.

4. CONCLUSIONS

The electrochemical behaviour of phenol, catechol, hydroquinone, resorcinol, and dopamine, and *para*-substituted phenolic compounds, 4-ethylphenol, and tyrosine, tyramine, was investigated by voltammetric techniques at GCE, in order to determine and identify the electroactive centre and the oxidation pathways of these compounds. The voltammetric behaviour of phenol was studied over a wide pH range, is irreversible, occurring in one step with the transfer of one electron and one proton, undergoes

hydrolysis and leads, in a EC mechanism, to two oxidation products, *ortho*-quinone and *para*-quinone, which are reversibly oxidised in a pH dependent mechanism.

The *para*-substituted phenolic compounds, 4-ethylphenol, tyramine and tyrosine, had different substituents at the position C4 of phenol, so they can only be oxidised in the *ortho* position to a catechol type species. They present one oxidation peak corresponding to the oxidation of phenol, adsorb on the electrode surface and further oxidation involves only a reversible peak instead of two for phenol. Taking into consideration all electrochemical studies performed, it can be concluded that the electrochemical behavior of these *para*-substituted phenolic compounds occurs in the phenol group and the EC mechanism was proposed.

5. ACKNOWLEDGEMENTS

Financial support from Fundação para a Ciência e Tecnologia (FCT), Ph.D. Grant SFRH/BD/37231/2007 (T.A. Enache), projects PTDC/QUI/65732/2006 and PTDC/QUI/098562/2008, POCI (co-financed by the European Community Fund FEDER), CEMUC-R (Research Unit 285), is gratefully acknowledged.

REFERENCES

[1] E. T. Denisov, I. B. Afanas'ev, Chemistry of Antioxidants in Oxidation and Antioxidants in Organic Chemistry and Biology, CRC Press Taylor & Francis Group 6000 Broken Sound Parkway NW, 2005, pp 488-500

[2] M. Valko, D. Leibfritz, J. Moncol, M.T.D. Cronin, M. Mazur, J. Telser, Free radicals and antioxidants in normal physiological functions and human disease, Int J Biochem Cell Biol. 39 (2007) 44–84

[3] M. Cristani, M. D'Arrigo, G. Mandalari, F. Castelli, M. G. Sarpietro, D. Micieli, D. Trombetta. Interaction of four monoterpenes contained in essential oils with model membranes: Implications for their antibacterial activity. J Agr Food Chem. 55 (2007) 6300-6308.

[4] L. De Martino, V. De Feo, F. Fratianni, F. Nazzaro, Chemistry, antioxidant, antibacterial and antifungal activities of volatile oils and their components, Nat Prod Lett. 4 (2009) 1741-1750.

[5] M. Sengul, H. Yildiz, N. Gungor, B.t Cetin, Z. Eser, S. Ercisli, Total phenolic content, antioxidant and antimicrobial activities of some medicinal plants, Pak. J. Pharm. Sci. 22 (2009) 102-106

[6] M.J.R. Vaquero, M.R. Alberto, M.C. Manca de Nadra, Antibacterial effect of phenolic compounds from different wines, Food Contr 18 (2007) 93-101.

[7] Z. Zhang, X.Y. Lian, S. Li, J.L. Stringer, Characterization of chemical ingredients and anticonvulsant activity of American skullcap (Scutellaria lateriflora), Phytomedicine 16 (2008) 485-493.

[8] L.R.C. Barclay, C.E. Edwards, M.R. Vinqvist, Media Effects on Antioxidant Activities of Phenols and Catechols, J. Am. Chem. Soc. 121 (1999) 6226–6231.

[9] M.A. Soobrattee, V.S. Neergheen, A. Luximon-Ramma, O.I. Aruoma, T. Bahorun, Phenolics as potential antioxidant therapeutic agents: mechanism and actions, Mutat Res. 579 (2005) 200-213.

[10] M. Leopoldini, T. Marino, N. Russo, M. Toscano, Antioxidant Properties of Phenolic Compounds: H-Atom versus Electron Transfer Mechanism, J. Phys. Chem. A. 108 (2004) 4916-4922.

[11] D.M. Pereira, P. Valentão, J. A. Pereira, P.B. Andrade, Phenolics: From Chemistry to Biology, Molecules 14 (2009) 2202-2211;

[12] B. Malfoy, J.A. Reynaud, Electrochemical investigations of amino acids at solid electrodes. Part II: Amino acids containing no sulphur atoms: Tryptophan, tyrosine, histidine and derivatives, J. Electroanal. Chem. 114 (1980) 213-223

[13] J.A. Reinaud, B. Malfoy, A. Bere, The electrochemical oxidation of three proteins: RNAase A, bovine serum albumin, and concavalin A at solid electrodes, J. Electroanal. Chem. 116 (1980) 595-606

[14] S. Andreescu, D. Andreescu, O.A. Sadik, A new electrocatalytic mechanism for the oxidation of phenols at platinum electrodes, Electrochem. Commun. 5 (2003) 681–688.

[15] V. Brabec, Electrochemical oxidation of nucleic acids and proteins at graphite electrode. Qualitative aspects, J. Electroanal. Chem. 116 (1980) 69-82

[16] P. Janeiro, A.M. Oliveira Brett, Catechin electrochemical oxidation mechanism, Anal. Chim. Acta. 518 (2004) 109-115

[17] I. Novak, M. Seruga, S. Komorsky-Lovric, Square wave and cyclic voltammetry of epicatechin gallate on glassy carbon electrode, J. Electroanal. Chem. 631 (2009) 71-75.

[18] J. L. Boudenne, O. Cerclier, J. Galéa, E. Van der Vlist, Electrochemical oxidation of aqueous phenol at a carbon slurry electrode, Appl. Catal. Gen. 143 (1996) 185-202.

[19] P. Janeiro, A. M. Oliveira Brett, Redox Behavior of Anthocyanins Present in Vitis vinifera L., Electroanalysis 19 (2007) 1779-1786.

[20] H. Notsu, T. Tatsuma, A. Fujishima, Tyrosinase-modified boron-doped diamond electrodes for the determination of phenol derivatives, J. Electroanal. Chem. 523 (2002) 86–92.

[21] J. Iniesta, P.A. Michaud, M. Panizza, G. Cerisola, A. Aldaz, Ch. Comninellis, Electrochemical oxidation of phenol at boron-doped diamond electrode, Electrochim. Acta. 46 (2001) 3573-3578.

[22] B. Nasr, G. Abdellatif, P. Canizares, C. Sáez, J. Lobato, M. A. Rodrigo, Electrochemical oxidation of hydroquinone, resorcinol, and catechol on boron-doped diamond, Environ. Sci. Technol. 39 (2005) 7234-7239

[23] J. L. Munñiz Álvarez, J. A. García Calzón, J. M. López Fonseca, , Square-wave voltammetry of the o-catechol–Ge(IV) catalytic system after adsorptive preconcentration at a hanging mercury drop electrode, Talanta 53 (2001) 721–731

[24] E. Chatzisymeon, S. Fierro, I. Karafyllis, D. Mantzavinos, N. Kalogerakis, A. Katsaounis, Anodic oxidation of phenol on Ti/IrO_2 electrode: Experimental studies, Catal. Today 151 (2010) 185-189.

[25] C.M.A. Brett, A.M. Oliveira Brett, Cyclic voltammetry and linear sweep techniques. In Electrochemistry. Principles, methods and applications, Oxford University Press, UK. 1993 pp 174-198

[26] P. Chen, R.L. McCreery, Control of electron transfer kinetics at glassy carbon electrodes by specific surface, Anal. Chem. 68 (1966) 3958-3965

[27] M. M. Baizer, Anodic oxidation of hydrquinones and catechols by Veron D. Parker. In Organic electrochemistry, Marcel Dekker INC., New York, USA 1973 pp 536-537

[28] S. Shahrokhian, S. Bozorgzadeh, Electrochemical oxidation of dopamine in the presence of sulfhydryl compounds: Application to the square-wave voltametric detection of penicillamine and cysteine, Electrochim. Acta 51 (2006) 4271.

Table 1. Supporting electrolytes, 0.1 M ionic strength.

pH	Composition
1.0	H_2SO_4
2.0	HCl + KCl
3.3	HAcO + NaAcO
4.2	HAcO + NaAcO
5.0	HAcO + NaAcO
6.0	NaH_2PO_4 + Na_2HPO_4
7.0	NaH_2PO_4 + Na_2HPO_4
8.0	NaH_2PO_4 + Na_2HPO_4
9.0	$NaHCO_3$ + NaOH
10.0	$NaHCO_3$ + NaOH
11.0	$NaHCO_3$ + NaOH
12.0	NH_3+NH_4Cl

FIGURES

Scheme 1. Chemical structure of phenol, catechol, hydroquinone, resorcinol, dopamine and *para*-substituted phenols.

Scheme 2. Oxidation mechanism: (A) phenol and (B) *para*-subtituted phenols.

Figure 1. CVs with baseline subtracted in pH 7.0 0.1 M phosphate buffer 30 μM phenol: (▬) first scan and (•••) second scan, $\nu = 50$ mV s^{-1}.

Figure 2. DP voltammograms of (▬) supporting electrolyte pH 7.0 0.2 M phosphate buffer and 25 μM phenol: (▬) first and (▬) second scan, and DP voltammograms baseline-corrected, (•••) first and (•••) second scan.

Figure 3. (A) 3D plot of DP voltammograms in 25 μM phenol and (B) Plot of phenol E_{p1} (■) and I_{p1} (○) vs. pH.

Figure 4. (A) 3D plot of second DP voltammograms in 25 μM phenol and (B) Plot of phenol oxidation products E_{p2} (■), E_{p3} (●), I_{p2} (□) and I_{p3} (○) vs. pH.

Figure 5. DP voltammograms baseline subtracted in pH 7.0 0.2 M phosphate buffer, (▬) first and (•••) second scans, for 25 μM: (A) phenol, (B) catechol, (C) hydroquinone and (D) resorcinol.

Figure 6. DP voltammograms baseline subtracted in pH 7.0 0.2 M phosphate buffer, (▬) first and (•••) second scans, for 25 μM: (A) 4-ethylphenol, (B) tyrosine, (C) tyramine and (D) dopamine.

Figure 7. SW voltammograms in pH 7.0 0.2 M phosphate buffer 25 μM: (A) first and (B) second scans of phenol, (C) first scan catechol, (D) first scan hydroquinone, (E) first and (F) second scans of resorcinol; f = 25 Hz, ΔE_s = 2 mV, v_{eff} = 50 mV s^{-1}, pulse amplitude 50 mV; I_t – total current, I_f – forward current, I_b – backward current.

Figure 8. SW voltammograms in pH 7.0 0.2 M phosphate buffer 25 μM: (A) first and (B) second scans of tyramine, and (C) first scan dopamine; f = 25 Hz, ΔE_s = 2 mV, v_{eff} = 50 mV s^{-1}, pulse amplitude 50 mV; I_t – total current, I_f – forward current, I_b – backward current.

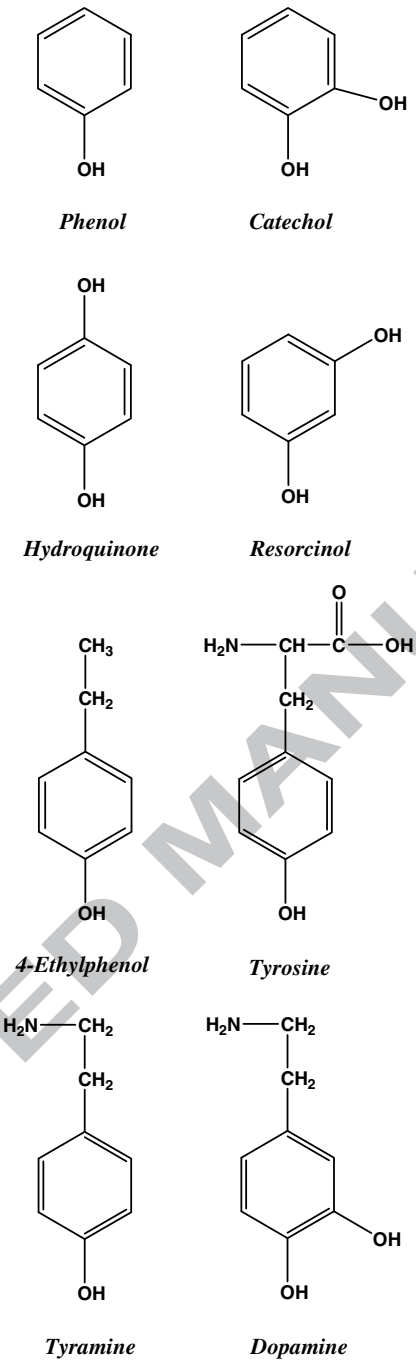

Scheme 1. Chemical structure of phenol, catechol, hydroquinone, resorcinol, dopamine and *para*-substituted phenols.

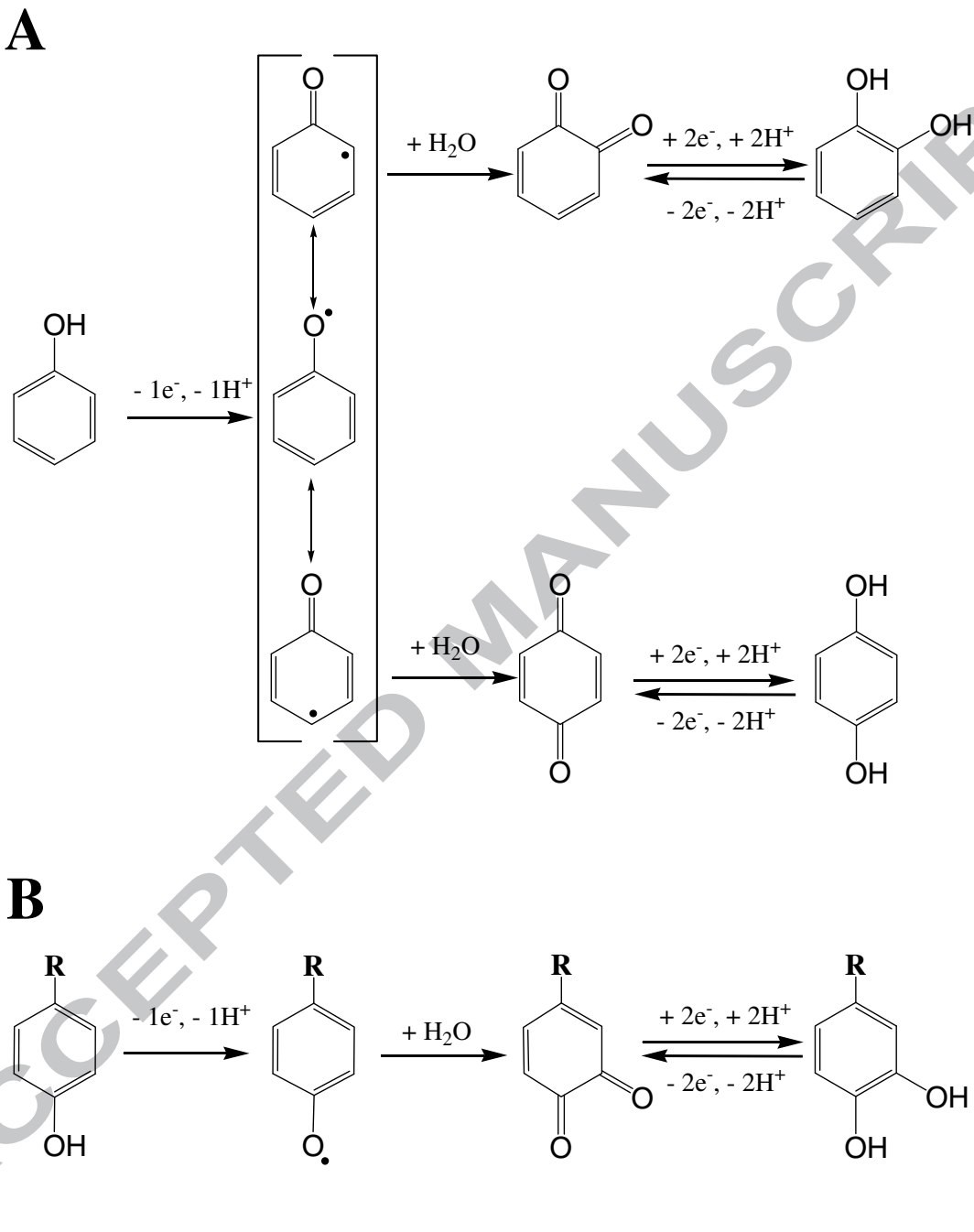

Scheme 2. Oxidation mechanism: (A) phenol and (B) *para*-subtituted phenols.

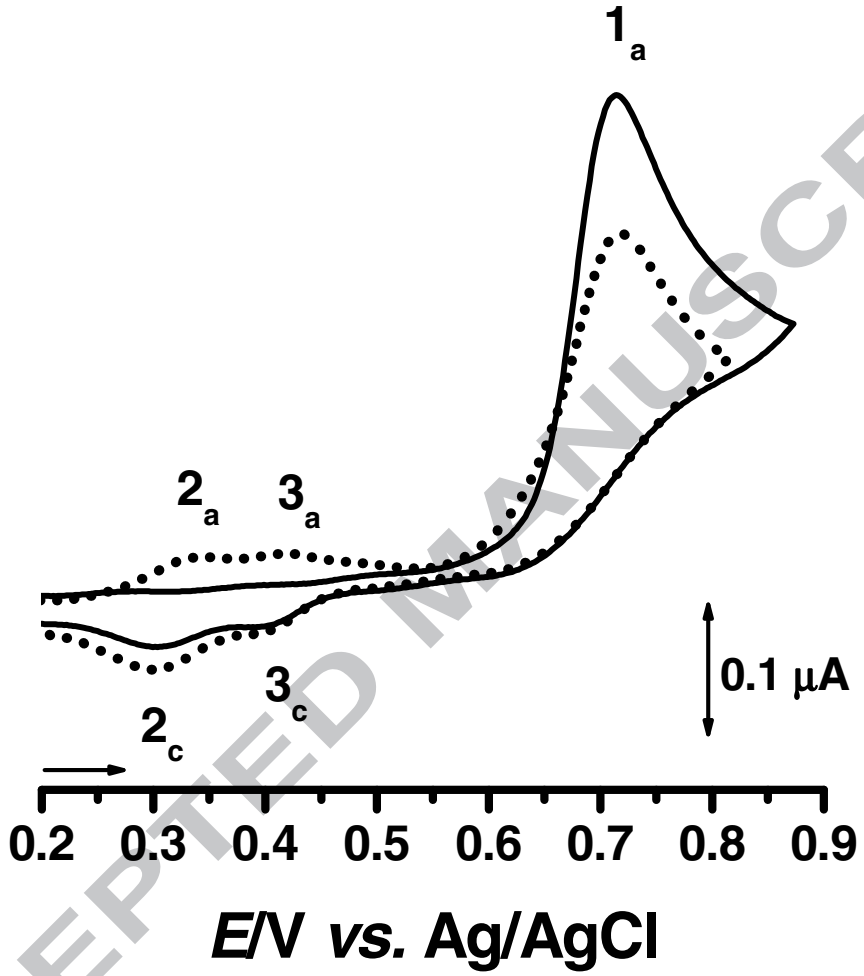

Figure 1. CVs with baseline subtracted in pH 7.0 0.1 M phosphate buffer 30 μM phenol: (—) first scan and (•••) second scan, ν = 50 mV s^{-1}.

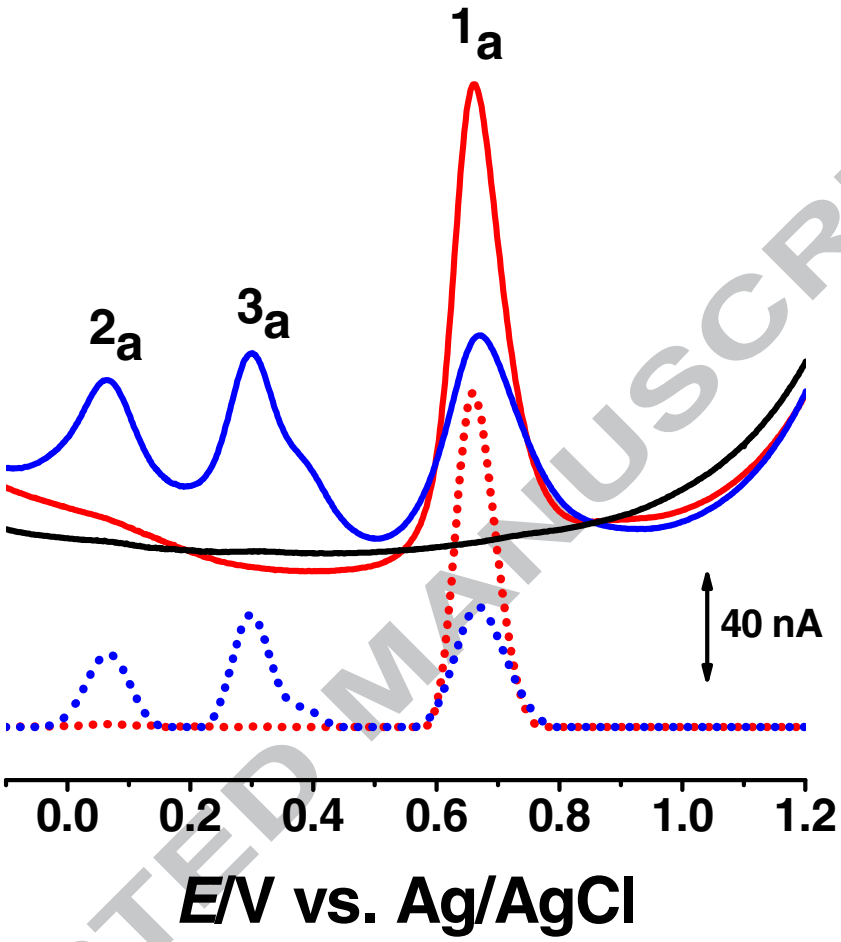

Figure 2. DP voltammograms of (—) supporting electrolyte pH 7.0 0.2 M phosphate buffer and 25 µM phenol: (—) first and (—) second scan, and DP voltammograms baseline-corrected, (•••) first and (•••) second scan.

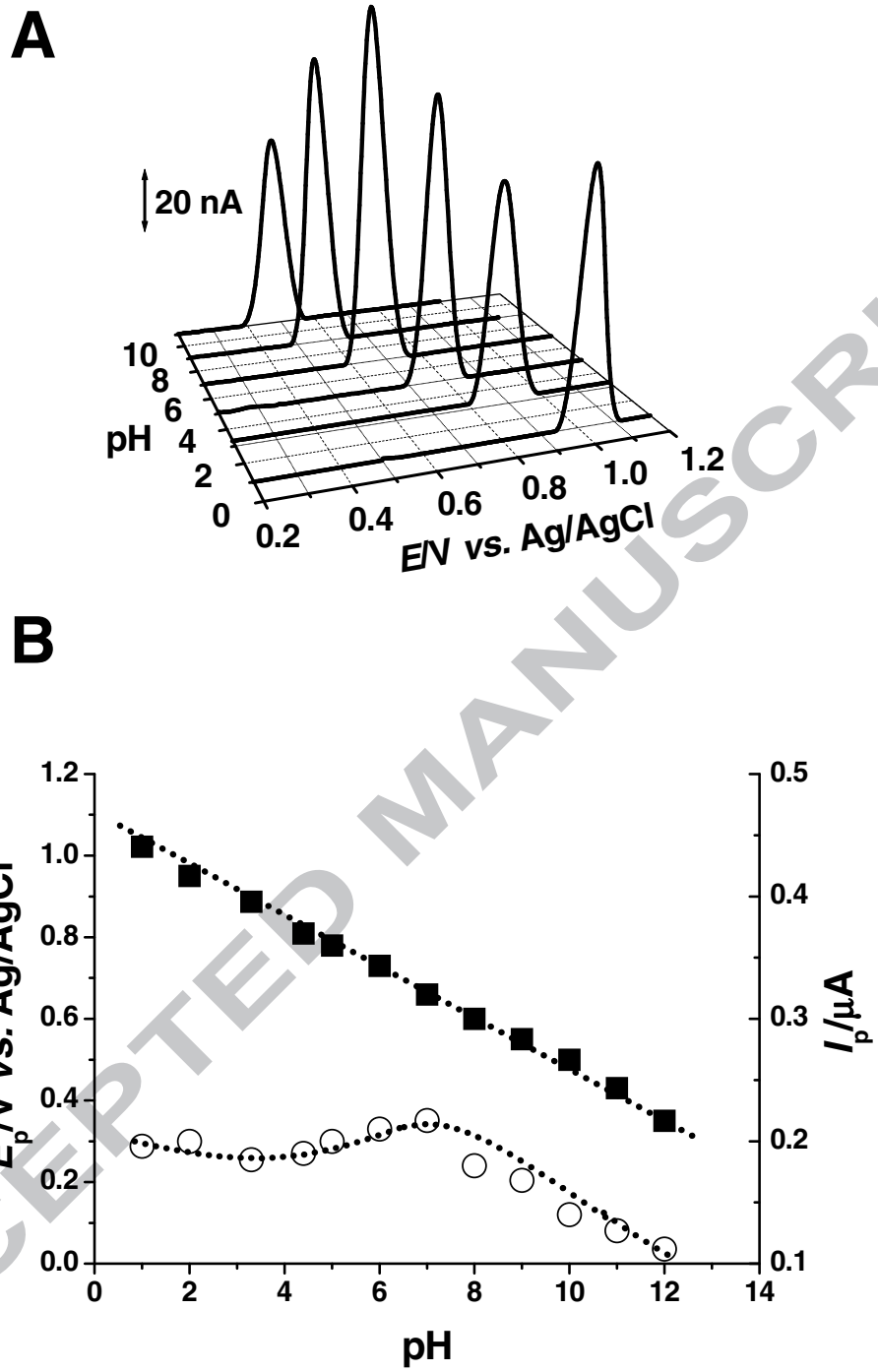

Figure 3. (A) 3D plot of DP voltammograms in 25 μM phenol and (B) Plot of E_{p1} (■) and I_{p1} (○) vs. pH.

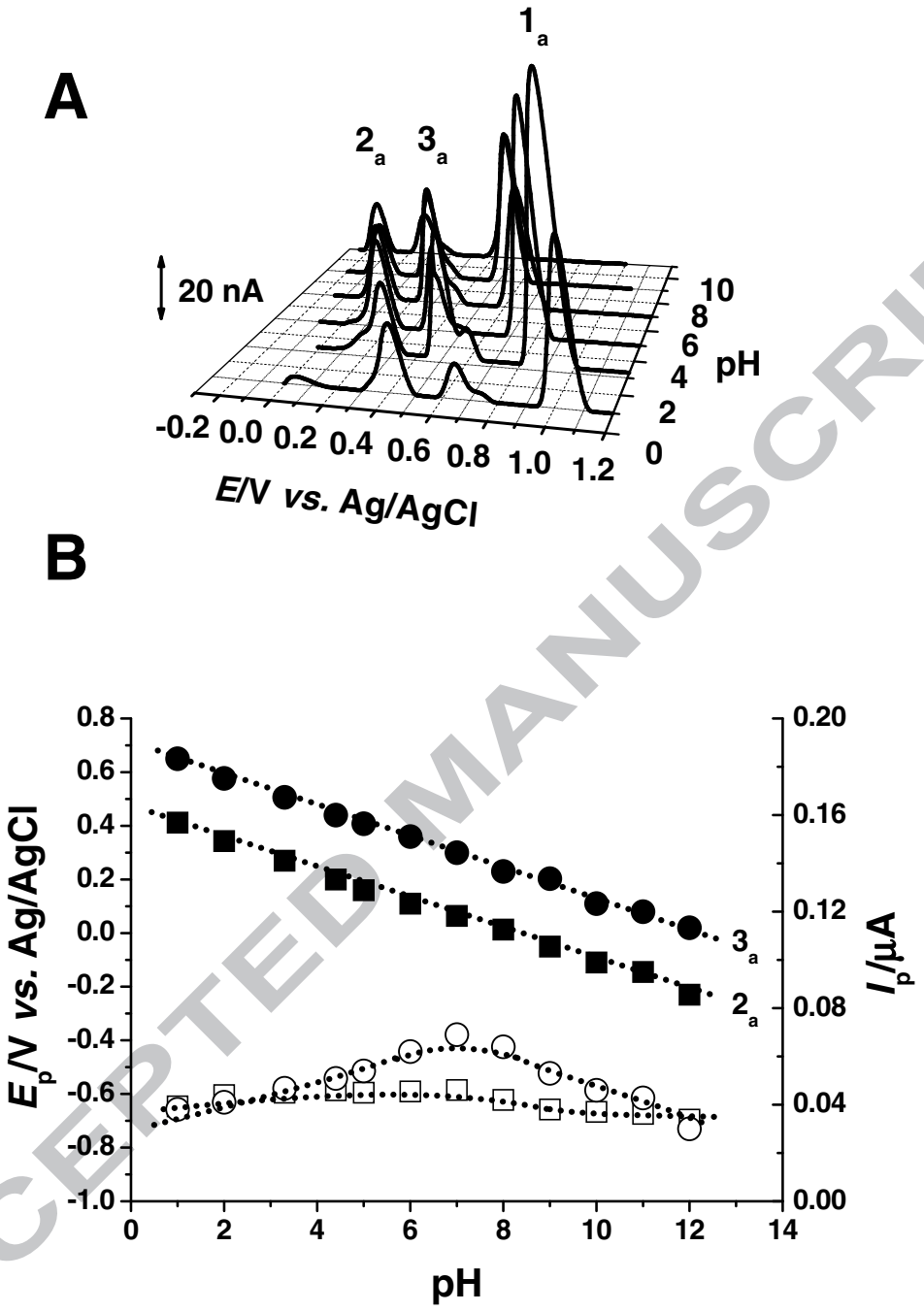

Figure 4. (A) 3D plot of second DP voltammograms in 25 μM phenol and

(B) Plot of phenol oxidation products E_{p2} (■),E_{p3} (●), I_{p2} (□) and I_{p3} (○) vs. pH.

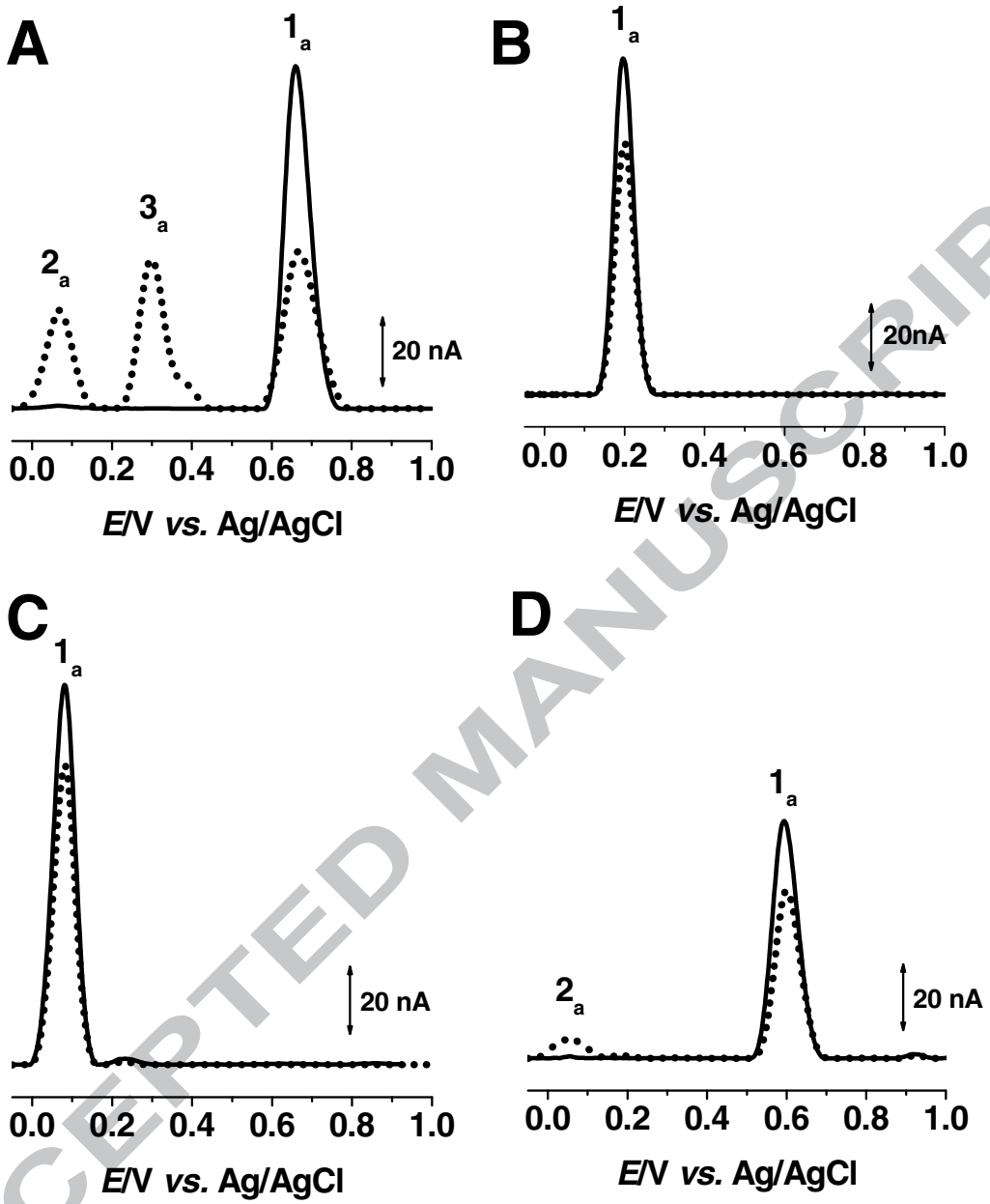

Figure 5. DP voltammograms baseline subtracted in pH 7.0 0.2 M phosphate buffer, (—) first and (•••) second scans, for 25 µM: (A) phenol, (B) catechol, (C) hydroquinone and (D) resorcinol.

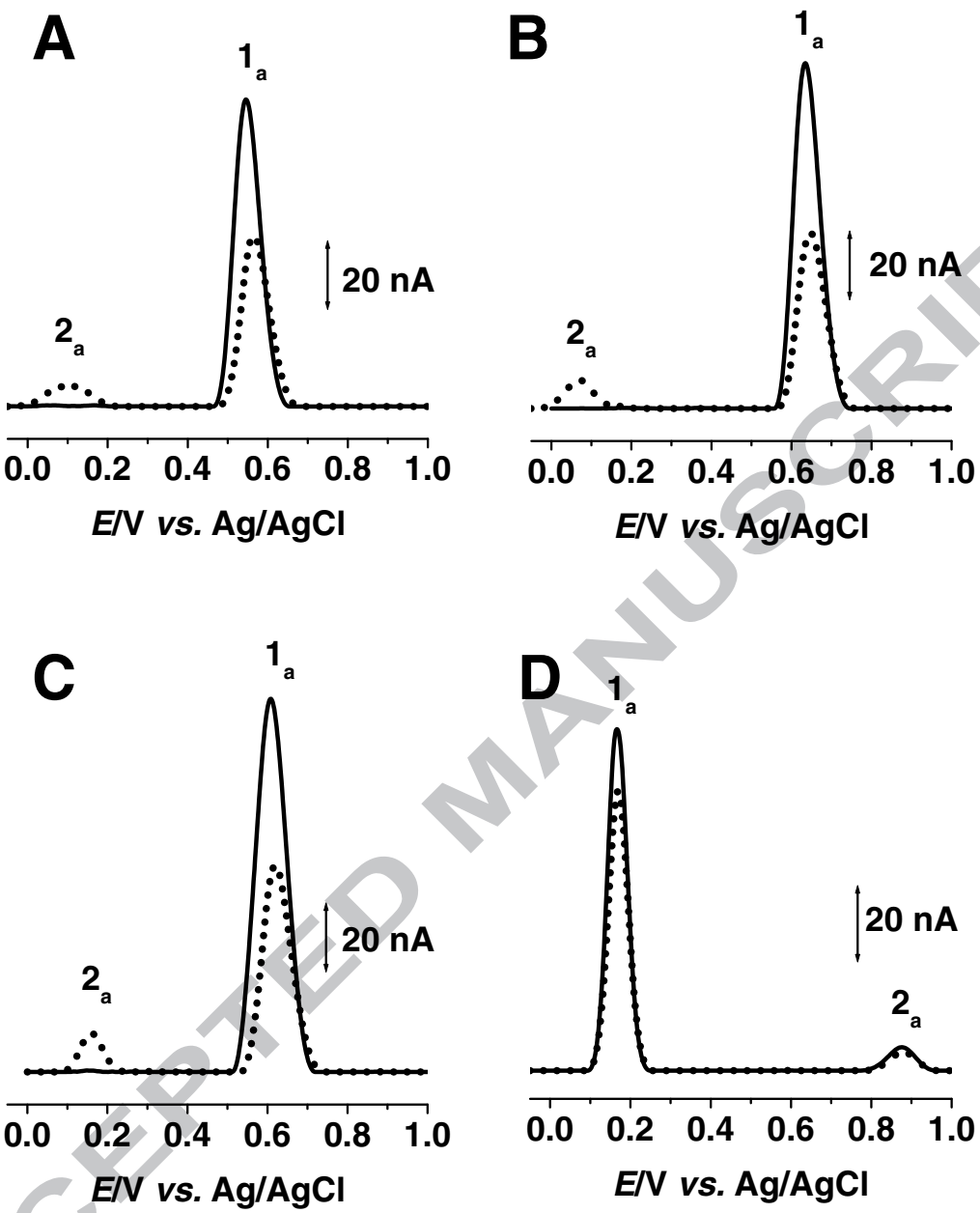

Figure 6. DP voltammograms baseline subtracted in pH 7.0 0.2 M phosphate buffer, (▬) first and (•••) second scans, for 25 μM: (A) 4-ethylphenol, (B) tyrosine, (C) tyramine and (D) dopamine.

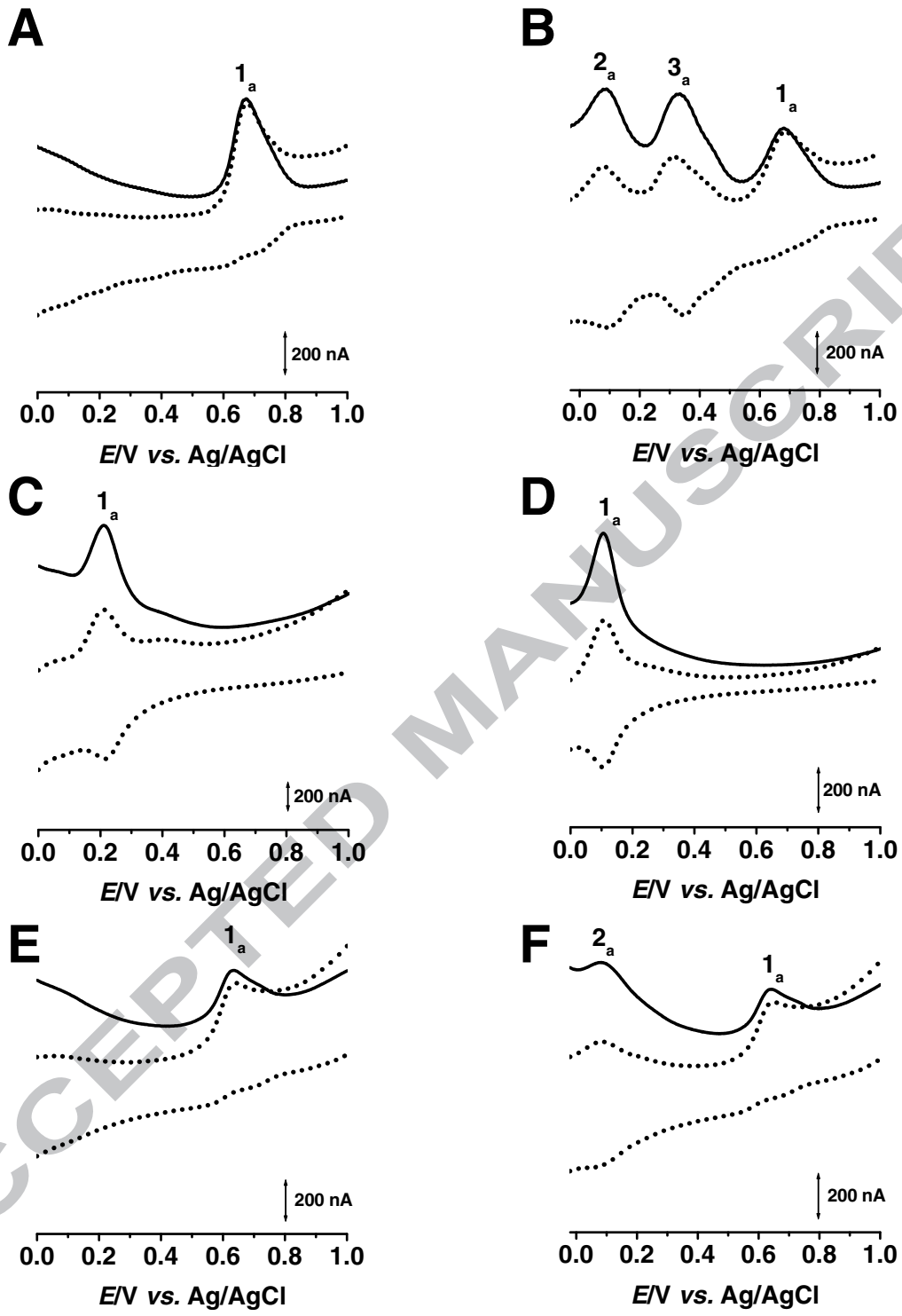

Figure 7. SW voltammograms in pH 7.0 0.2 M phosphate buffer 25 μM: (A) first and (B) second scans of phenol, (C) first scan catechol, (D) first scan hydroquinone, (E) first and (F) second scans of resorcinol; f = 25 Hz, ΔE_s = 2 mV, ν_{eff} = 50 mV s^{-1}, pulse amplitude 50 mV;I_t – total current, I_f – forward current, I_b – backward current.

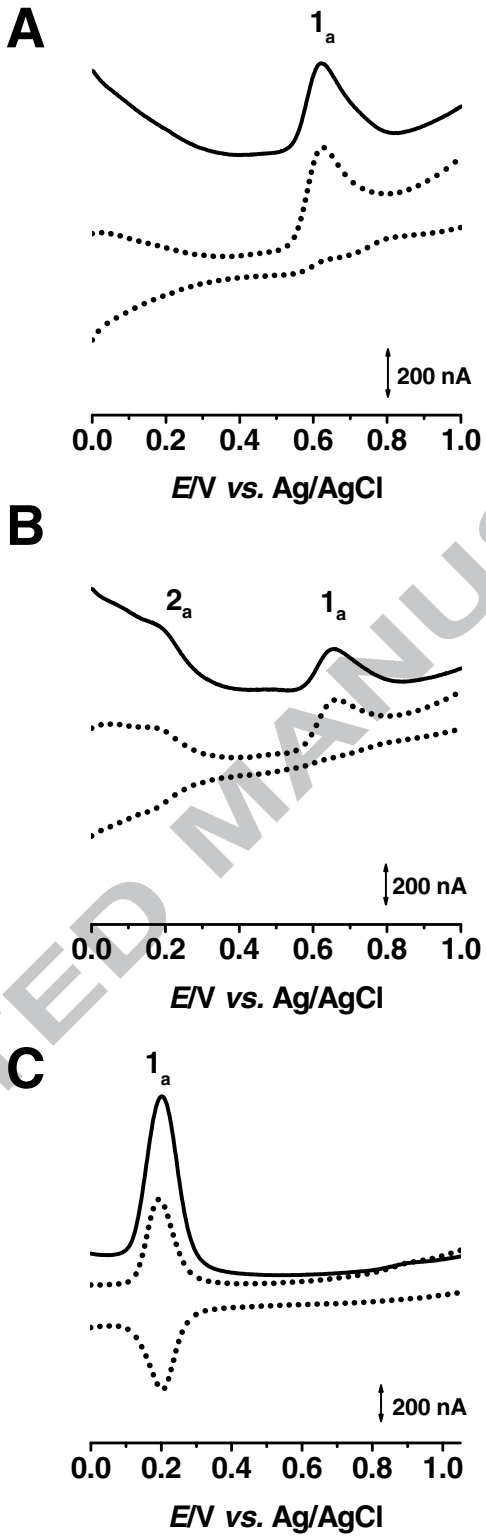

Figure 8. SW voltammograms in pH 7.0 0.2 M phosphate buffer 25 μM: (A) first and (B) second scans of tyramine, and (C) first scan dopamine; f = 25 Hz, ΔE_s = 2 mV, ν_{eff} = 50 mV s^{-1}, pulse amplitude 50 mV; I_t – total current, I_f – forward current, I_b – backward current.

Phenol and *para*-substituted phenols electrochemical oxidation pathways

Teodor Adrian Enache and Ana Maria Oliveira-Brett*

Departamento de Química, Faculdade de Ciências e Tecnologia, Universidade de Coimbra, 3004-535 Coimbra, Portugal

Highlights

- Clarify the electrochemical behaviour of phenol, catechol, hydroquinone, resorcinol, dopamine;
- Clarify the electrochemical behaviour of *para*-substituted phenolic compounds, 4-ethylphenol, tyrosine, and tyramine;
- Study of the electrochemical mechanistic behaviour of *para*-substituted phenols.